



**PARAMETRIC INVESTIGATION FOR SINGLE SIDED  
AND DOUBLE SIDED FRICTION STIR WELDING OF  
ALUMINUM ALLOY 6061-T6 AND S275JR MILD STEEL  
BUTT JOINT**

by

**WAN MOHD SYAFIQ BIN WAN SULONG  
(1441411479)**

A thesis submitted in fulfillment of the requirements for the degree of  
Doctor of Philosophy

**School of Mechatronic Engineering  
UNIVERSITI MALAYSIA PERLIS**

2019

## ACKNOWLEDGMENT

In the name of Allah, the Most Gracious and the Most Merciful. Alhamdulillah, all praises to Allah for the strengths and His blessing in completing this project. Indeed, He is the Most Powerful, the Subduer and the Bestower above all. My deepest gratitude goes to my beloved parents; Mr. Wan Sulong Bin Wan Omar and Mrs. Nor Aishah Binti Mokhtar for their greatest support and consistent du'as for this achievement.

I would like to express my appreciation to the Dean of School of Mechatronic Engineering, Dr. Muhammad Juhairi Aziz Bin Safar as well as the former Dean PM Ir. Dr. Abu Hassan Bin Abdullah for their encouragements throughout my research work. I would like to extend my profound gratefulness to my supervisor, Ts. Dr. Mohd Afendi Bin Rojan for his ideas, invaluable guidance, continuous encouragement and constant support in making this project possible. I am greatly indebted for his inspiration and thirst for knowledge and research, which helped me to groom and nurture myself throughout my research work. His continuous motivation to explore things helped me to complete my research successfully. I appreciate his consistent support from the first day I applied to graduate program to these concluding moments.

I am grateful to my co-supervisor, PM Dr. Mazlee Bin Mohd Noor for his guidance and support in the field of materials. Under his guidance and supervision, the materials investigation side of the research was accomplished successfully. I would also like to pay my appreciation to my co supervisor, PM Ir. Dr Ruslizam Bin Daud for his support and advice especially on the fracture behavior of materials.

Last but not least, sincere thanks to all those who directly or indirectly helped me at various stages of my research. Thank you for the kindness and moral support during the research.

## TABLE OF CONTENTS

	<b>PAGE</b>
DECLARATION OF THESIS	i
TABLE OF CONTENTS	ii
LIST OF TABLES	vii
LIST OF FIGURES	ix
LIST OF ABBREVIATIONS	xviii
LIST OF SYMBOLS	xix
ABSTRAK	xx
ABSTRACT	xxii
CHAPTER 1 : INTRODUCTION	1
1.1 Research Background	1
1.2 Problem Statement	6
1.3 Objective	9
1.4 Scope of Work	10
1.5 Organization of the Dissertation	11
CHAPTER 2 : LITERATURE REVIEW	13
2.1 Friction Stir Welding	14
2.1.1 Introduction	14
2.1.2 Zones	18

2.1.3	Material flow at advancing side and retreating side	19
2.1.4	Advantages of FSW	19
2.1.5	Current FSW innovations	20
2.1.6	Tool design	22
2.2	FSW: Aluminum and Steel	23
2.2.1	Influence of tool offset	30
2.2.2	Influence of tool rotational speed	34
2.2.3	Influence of tool travel speed	36
2.2.4	Influence of tool plunge depth	39
2.2.5	Influence of tool tilt angle	41
2.2.6	Influence of tool rotation	43
2.3	Defects and Issues of FSW	44
2.3.1	Tunnel defects	45
2.3.2	Steel fragments	47
2.3.3	Flash	48
2.3.4	Insufficient bonding	50
2.3.5	Tool life	51
2.4	Temperature during FSW	53
2.5	Microstructure of FSW joints	54
2.6	Hardness	56
2.7	IMC Layer	58

2.7.1	IMC Formation Theories	59
2.7.2	IMC thickness	61
2.8	Double Sided FSW	64
2.8.1	Mechanical properties	64
2.8.2	Microstructure	66
2.8.3	Hardness	68
2.9	Summary	68
CHAPTER 3 : METHODOLOGY		71
3.1	Introduction	71
3.2	Flow of Research Methodology	71
3.3	Material of welded plates and FSW tool	73
3.4	Weld Machine and Procedure	76
3.4.1	Jig designs	76
3.4.2	Welding procedure and list of joints	80
3.5	Specimen extraction and testing	81
3.6	Testing and Analysis	85
3.7	Temperature Measurement	87
CHAPTER 4 : RESULTS & DISCUSSION		89
4.1	Effects of welding parameters on defect, microstructure and tensile strength	89
4.1.1	Parametric Study	90
4.1.1.1	Tool Offset	90

4.1.1.2	Tool Rotation	93
4.1.1.3	Tool Plunge Depth	95
4.1.1.4	Tool Travel Speed	106
4.1.1.5	Tool Tilt Angle	115
4.1.1.6	Summary	122
4.1.2	Relationship between parameters and defects	123
4.1.2.1	Flash	124
4.1.2.2	Tunnel Defect	125
4.1.2.3	Insufficient Joining	126
4.1.2.4	Deformed tool	129
4.1.2.5	Root defect	133
4.1.3	Relationship between parameters and microstructure	139
4.1.3.1	IMC Layer	139
4.1.3.2	Grain size	142
4.1.4	Microhardness	148
4.1.5	Tensile Strength	151
4.1.6	Summary	158
4.2	Influence of Tool Pin Length on Double Sided FSW between AA6061-T6 and S275JR mild steel	162
4.2.1	Macrostructure	162
4.2.2	Temperature Measurement	164
4.2.3	Microstructure	167

4.2.3.1	Grain size	167
4.2.3.2	IMC Layer	173
4.2.4	Microhardness	184
4.2.5	Tensile Strength	189
4.2.6	Reversing advancing and retreating sides during 2 <sup>nd</sup> side welding	192
4.2.7	Summary	194
CHAPTER 5 : CONCLUSION		196
5.1	Conclusion	196
5.2	Suggestions for Future Work	198
REFERENCE		200
APPENDIX A: AA6061-T6 FSW DATA		217
LIST OF PUBLICATIONS		218

## LIST OF TABLES

		<b>PAGE</b>
Table 2.1	Most commonly cited aluminum-to-steel FSW papers	24
Table 2.2	Tool offset study findings in aluminum-to-steel FSW	33
Table 2.3	Tool rotational speed study findings in aluminum-to-steel FSW	36
Table 2.4	Tool travel speed study findings on aluminum-to-steel FSW	38
Table 2.5	Tool plunge depth study findings on aluminum-to-steel FSW	40
Table 2.6	Tool tilt angle study findings on aluminum-to-steel FSW	43
Table 3.1	Chemical compositions of base metals AA6061-T6 and S275JR	74
Table 3.2	Mechanical properties of base metals AA6061-T6 and S275JR	74
Table 3.3	Chemical composition of ASSAB 8407 Supreme taken from data sheet	75
Table 3.4	List of welded joints and their respective welding parameters	81
Table 4.1	IMC layer thickness at locations A, B and C of joints SS4 and SS14	121
Table 4.2	Highlights of parametric study findings	122
Table 4.3	Root defect width observed on fracture surface of tensile specimens extracted from FSW joints	135

Table 4.4	List of each joints with its respective parameter and ultimate tensile strength (UTS) value	152
Table 4.5	List of each joints and its respective parameters, root defect presence and UTS	153
Table 4.6	Fracture location and UTS of tensile specimens of welded joints	189

@This item is protected by original copyright

## LIST OF FIGURES

	<b>PAGE</b>	
Figure 2.1	(a) Schematic diagram of friction stir welding. (b) Side view of schematic diagram	15
Figure 2.2	Axial pressing force and lateral moving force during plunging, dwelling and welding stages	17
Figure 2.3	Cross sectional view of typical microstructure regions of a FSW joint (adapted from N. Kumar & Mishra, 2014)	18
Figure 2.4	Illustrations of the definitions of (a) tool offset and (b) tool axis offset	31
Figure 2.5	Tunnel defect in an aluminum-to-steel FSW joint (adapted from Dehghani, Amadeh, et al., 2013)	46
Figure 2.6	Steel fragments and voids observed in AA5083-H321 and 316L stainless steel FSW joint (Yazdipour & Heidarzadeh, 2016)	48
Figure 2.7	Cross-section of excessive material flash on ADC12 aluminum FSW joint (Kim et al., 2006)	49
Figure 2.8	Unstirred zone at the root of AA6013-T4 to X5CrNi18-10 stainless steel FSW joint denoted by letter “h” (Uzun et al., 2005)	51
Figure 2.9	Cracks observed at the root of AA6061-T6511 to TRIP 780/800 steel FSW joint (S. Zhao et al., 2018)	51
Figure 2.10	Microhardness profile of AA5083-H321 to 316L stainless steel FSW joint (Yazdipour & Heidarzadeh, 2016)	57
Figure 2.11	Al-Fe binary phase diagram (Baker, 1992)	60

Figure 2.12	Comparison of IMC layer thickness before and after heat treatment (Naumov et al., 2017)	62
Figure 3.1	Flow chart of research methodology	73
Figure 3.2	Grains of base metals (a) AA6061-T6 and (b) S275JR	74
Figure 3.3	Schematic drawing of FSW tool	75
Figure 3.4	(a) Appearance of FSW tool with pin length 4.5 mm, (b) All FSW tools with varying pin lengths	76
Figure 3.5	Milling machine used to perform FSW	77
Figure 3.6	(a) Dimension of base metal plates to be welded (b) allocated space for plates in jig (c) welded joint in clamped position (d) joint removed from Jig 1	78
Figure 3.7	(a) Dimension of base metal plates to be welded (b) Jig 2 with welded joint in clamped position (c) joint removed from Jig 2	79
Figure 3.8	(a) Location of tensile and microstructure specimens on joint Jig 1, (b) Dimension of tensile specimen size S1	84
Figure 3.9	(a) Location of tensile and microstructure specimens on joint Jig 2, (b) Dimension of tensile specimen size S2	84
Figure 3.10	(a) Image of grinder polisher machine (b) Polished microstructure sample	84
Figure 3.11	Extracted tensile specimens of size S1 and S2	86
Figure 3.12	(a) Universal testing machine (b) Vickers microhardness tester	86
Figure 3.13	(a) Optical Microscope and (b) Scanning Electron Microscope used for microstructural observations	87

Figure 3.14	Side view schematic drawing of thermocouple placement in the aluminum alloy plate	88
Figure 4.1	(a) Visible line seen on joint SS1 after welding. (b) Plates detached soon after welding	91
Figure 4.2	Steel fracture surfaces of tensile specimens from (a) SS2 and (b) SS3	92
Figure 4.3	(a) Excessive flash and surface breaking tunnel seen in joint SS5 (b) Tool wear observed after welding	92
Figure 4.4	Surface appearance of joint SS4	93
Figure 4.5	(a) Surface appearance of joint SS6 (b) Joint detached after welding	94
Figure 4.6	Schematic drawing of welding configuration where: (a) aluminum is placed at retreating side, and (b) aluminum is placed at advancing side	94
Figure 4.7	Surface appearances of joints (a) SS7, (b) SS4, (c) SS8 and (d) SS9	96
Figure 4.8	Illustration of the effect of (a) lower and (b) higher tool plunge depth on the width of affected zone	96
Figure 4.9	Cross sections of joints (a) SS7, (b) SS4, (c) SS8 and (d) SS9	98
Figure 4.10	Illustration of the effect of (a) low and (b) high tool plunge depth on the width of plunged shoulder	98
Figure 4.11	SEM images of the cross sections of joints (a) SS7, (b) SS4, (c) SS8 and (d) SS9	101
Figure 4.12	SEM images of IMC layer at the crown of joints (a) SS7, (b) SS4, (c) SS8 and (d) SS9	102

Figure 4.13	SEM images of IMC layer at the middle region of joints (a) SS7, (b) SS4, (c) SS8 and (d) SS9	102
Figure 4.14	IMC layer thickness against tool plunge depth used during FSW	103
Figure 4.15	Grains at the SZ of joints (a) SS7, (b) SS4, (c) SS8 and (d) SS9	104
Figure 4.16	Average grain size in the SZ against tool plunge depth used during FSW	105
Figure 4.17	Temperature against time plots of joints SS4, SS7 and SS9	106
Figure 4.18	Surface appearances for joints (a) SS10, (b) SS4, (c) SS11 and (d) SS12	107
Figure 4.19	Cross sections of joints (a) SS10, (b) SS4, (c) SS11 and (d) SS12	108
Figure 4.20	SEM images of cross sections of joints (a) SS10, (b) SS4, (c) SS11 and (d) SS12	110
Figure 4.21	SEM images of IMC layer at the crown of joints (a) SS10, (b) SS4, (c) SS11 and (d) SS12	111
Figure 4.22	SEM images of IMC layer at the middle region of joints (a) SS10, (b) SS4, (c) SS11 and (d) SS12	112
Figure 4.23	IMC layer thickness against tool travel speed used during FSW	112
Figure 4.24	Grains at the SZ of joints (a) SS10, (b) SS4, (c) SS11 and (d) SS12	114
Figure 4.25	Average grain size in the SZ against tool travel speed used during FSW	114

Figure 4.26	Temperature against time plots of joints SS10, SS4 and SS12	115
Figure 4.27	Surface appearances of joints (a) SS13, (b) SS13 which detached prior to machining, (c) SS4 and (d) SS14	117
Figure 4.28	Illustration of the effect of (a) 1°, (b) 3° and (c) 5° tool tilt angle on the affect zone	117
Figure 4.29	(a) Cross section of joint 1 TT. (b) Cross section image of detached joint 5 TT	118
Figure 4.30	SEM images of cross sections of joints (a) SS14 and (b) SS4. Red boxes indicate locations of zoomed in figures	119
Figure 4.31	Zoomed in SEM images of IMC layer on the interface of joints ((a), (c), (e)) SS14 and ((b), (d), (f)) SS4 at postions A, B, and C	120
Figure 4.32	Grains at SZ of joint welded with SS14	121
Figure 4.33	Temperature against time plots of joints SS13, SS4 and SS14	122
Figure 4.34	(a) Surface defect and excessive material flash on joint SS5, (b) Excessive material flash on joint SS9, (c) Excessive material flash on joint SS13	125
Figure 4.35	(a) Flat faying surface of detached steel and aluminum of joint SS6. (b) SEM image of the flat steel faying surface	128
Figure 4.36	(a) Steel fracture surface of joint SS3. (b) and (c) are SEM images of Region A and B respectively	129
Figure 4.37	(a) Original shape of cylindrical tool pin (b) Deformed tool pin in a truncated conical shape	130

Figure 4.38	(a) Deformed tool shoulder with some built up aluminum residue. (b) Deformed tool shoulder with critical level of aluminum residue	132
Figure 4.39	Weld surface of a joint welded using an uncleaned FSW tool	132
Figure 4.40	Tool shoulder appearance after aluminum residue was removed	133
Figure 4.41	Image of steel fracture surface of joint SS4's tensile specimen	134
Figure 4.42	Steel fracture surfaces of tensile specimens taken from joints (a) SS4, (b) SS7, (c) SS8, (d) SS9, (e) SS10, (f) SS11, (g) SS12 and (h) SS14	135
Figure 4.43	SEM observation of steel fracture surface of SS4's tensile specimen: (a) Region A and (b) Region B	136
Figure 4.44	(a) SEM image of SS4's cross section (b) Zoomed in image of interface at location specified by red box in Figure 4.36a	136
Figure 4.45	Steel fracture surface of tensile specimen from joint welded with tool pin length of 4.8 mm	138
Figure 4.46	SEM observation of steel fracture surface of tensile specimen from 4.8 PL: (a) Region A and (b) Region B	139
Figure 4.47	Average IMC layer thickness at the (a) crown and (b) middle region of joints	141
Figure 4.48	Average grain size ( $\mu\text{m}$ ) at the SZ of joints welded with different parameters	143
Figure 4.49	Grains at the TMAZ of joints (a) SS4, (b) SS7, (c) SS8, (d) SS9, (e) SS10, (f) SS11, (g) SS12 and (h) SS14	145

Figure 4.50	Average grain size ( $\mu\text{m}$ ) at the TMAZ of joints welded with different parameters	146
Figure 4.51	Grains at the HAZ of joints (a) SS4, (b) SS7, (c) SS8, (d) SS9, (e) SS10, (f) SS11, (g) SS12 and (h) SS14	147
Figure 4.52	Average grain size ( $\mu\text{m}$ ) at the HAZ of joints welded with different parameters	147
Figure 4.53	Microhardness profiles for joints with varied (a) tool plunge depth, (b) tool travel speed and (c) tool tilt angle	150
Figure 4.54	(a) Tensile specimen from SS8* fracturing at interface. (b) Tensile specimen from SS11* fracturing at the aluminum HAZ. (c) Steel fracture surface of tensile specimen from SS8*.	155
Figure 4.55	SEM image of aluminum fracture surface when sample fractured at (a) interface of SS8* and (b) aluminum HAZ of SS11*	155
Figure 4.56	(a) UTS vs IMC layer thickness at the crown, (b) UTS vs IMC layer thickness at the middle region of joints	157
Figure 4.57	Fracture of tensile specimens from joint (a) SS7, (b) SS12 and (c) SS10	158
Figure 4.58	Cross sections of welds (a) DS1, (b) DS2, (c) DS3, (d) DS4. All figures are oriented such that top surface of 1 <sup>st</sup> side welding is always at the top	163
Figure 4.59	Temperature against time plots for joints (a) DS1, (b) DS2, (c) DS3 and (d) DS4	166
Figure 4.60	Grains at SZ and respective grain sizes of samples (a) SS4, (b) DS1, (c) DS2, (d) SS15, (e) DS3 untouched 1st side, (f) DS3 and (g) DS4	169

Figure 4.61	Grains at TMAZ and respective grain sizes of joints (a) SS4, (b) DS1, (c) DS2, (d) DS3 and (e) DS4	170
Figure 4.62	Grains at HAZ and respective grain sizes of joints (a) SS4, (b) DS1, (c) DS2, (d) DS3 and (e) DS4	171
Figure 4.63	Average grain size ( $\mu\text{m}$ ) at SZ, TMAZ and HAZ of DS-FSW joints welded with different tool pin lengths	171
Figure 4.64	SEM images of the cross sections of welds (a) SS4, (b) DS1, (c) DS2, (d) DS3, (e) DS4	174
Figure 4.65	SEM images of SS4's IMC layer at (a) Crown, (b) Top, (c) Mid A, (d) Mid B, (e) Mid C and (f) Root	177
Figure 4.66	SEM images of DS1's IMC layer at (a) Crown 1, (b) Top 1, (c) Mid 2, (d) Top 2 and (e) Crown 2	178
Figure 4.67	SEM images of DS2's IMC layer at (a) Crown 1, (b) Top 1, (c) Mid 1, (d) Mid-T 1, (e) Mid 2, (f) Top 2 and (g) Crown 2	179
Figure 4.68	SEM images of DS3's IMC layer at (a) Crown 1, (b) Top 1, (c) Mid 1, (d) Mid-T 1, (e) Mid 2, (f) Top 2 and (g) Crown 2	180
Figure 4.69	SEM images of DS4's IMC layer at (a) Crown 1, (b) Top 1, (c) Mid 1, (d) Mid-T 1, (e) Mid 2, (f) Top 2 and (g) Crown 2	181
Figure 4.70	Summary of IMC thickness at the interface from top to bottom of joints: (a) SS4.5, (b) DS4.5, (c) DS4, (d) DS3.5, and (e) DS3	182
Figure 4.71	SEM-EDS analysis at (a) DS3.5, (b) DS3.5 and (c) SS4.	184
Figure 4.72	Plots of microhardness profiles for joints (a) SS4, (b) DS1, (c) DS2, (d) DS3 and (e) DS4	188

Figure 4.73	Steel fracture surfaces of tensile specimen from (a) DS1 and (b) DS2	190
Figure 4.74	Fractured tensile specimens from (a) DS3 and (b) DS4	191
Figure 4.75	Image of sample DS5 that failed during machining	192
Figure 4.76	Image of tunnel defect observed in DS5	194

@This item is protected by original copyright

## LIST OF ABBREVIATIONS

IMC	Intermetallic Compound
FSW	Friction Stir Welding
TWI	The Welding Institute
SSFSW	Stationary Shoulder Friction Stir Welding
FSLW	Friction Stir Lap Welding
UTS	Ultimate Tensile Strength
USE-FSW	Ultrasound Enhanced Friction Stir Welding
FSD	Friction Stir Dovetailing
RHA	Rolled Homogeneous Armor
AS	Advancing Side
RS	Retreating Side
HSLA	High Strength Low Alloy
SZ	Stir Zone
TMAZ	Thermomechanically Affected Zone
HAZ	Heat Affected Zone
BM	Base Metal
UFSW	Underwater Friction Stir Welding
RDRFSW	Reverse Dual Rotation Friction Stir Welding
TO	Tool Offset
PD	Plunge Depth
TT	Tool Tilt
EHF	Effective Heat of Formation
HIF	Heat Input Factor
SS-FSW	Single Sided Friction Stir Welding
DS-FSW	Double Sided Friction Stir Welding
ASTM	American Society for Testing and Materials
OM	Optical Microscope
SEM	Scanning Electron Microscope
BSE	Backscattered Electron
EDS	Energy-Dispersive X-ray Spectroscopy

## LIST OF SYMBOLS

$A_t$	Thickness of Aluminum Alloy Plate
$S_t$	Thickness of Steel Plate
$\omega$	Tool rotational speed
$V$	Tool travel speed
$Z$	Zener-Holloman parameter
$\varepsilon'$	Strain rate
$Q$	Activation energy
$R$	Gas constant
$T$	Temperature
$q$	Heat input per unit time
$\mu$	Friction coefficient
$P$	Downwards pressure
$R_{sh}$	Tool shoulder radius
$V_v$	Volume of void
$k$	Proportional factor related to metal properties and temperature
$R_p$	Tool pin radius
$\tau$	Frictional shear stress
$H_p$	Tool pin length
$D_r$	Conical pin root radius
$D_t$	Conical pin tip radius
$D_s$	Shoulder diameter

## Penyiasatan Parametrik Kimpalan Kacau Geseran Aloi Aluminium 6061-T6 dan Keluli Lembut S275JR Dalam Sambungan Temu

### ABSTRAK

Kimpalan aduk geseran (FSW) adalah teknik sambungan keadaan pepejal yang mampu menyambung aluminium dan keluli bersama, dan memberi manfaat kepada industri-industri seperti automotif, aeroangkasa dan kimia kerana kekuatan tinggi dan keliatan keluli serta sifat tahan hakisan dan ketumpatan rendah aloi aluminium. Bagaimanapun, gabungan kedua-dua bahan bersama ini sukar kerana kecenderungan kuat untuk membentuk sebatian antara logam (IMC) rapuh dan keras pada antara muka aluminium dan keluli akibat resapan bersama semasa kimpalan. Walaupun pertumbuhan lapisan IMC diminimakan dalam FSW kerana suhu proses rendah, penyiasatan mengenai pengaruh parameter kimpalan pada pembentukan lapisan IMC serta sifat sendi lain seperti kekuatan tegangan dan kekerasan diperlukan. Kemunculan kecacatan berkaitan FSW seperti kecacatan terowong, ketidakcukupan kimpalan dan kecacatan akar juga perlukan perhatian kerana kesan negatifnya terhadap kekuatan sendi. Pengaruh FSW dwibelah (DS-FSW) pada sifat sendi aluminium-ke-keluli serta keupayaannya untuk memperbaiki kecacatan akar juga memerlukan penilaian. Beberapa parameter kimpalan telah dikaji dan kesannya terhadap sifat-sifat sendi disiasat: ofset alat, arah putaran alat, kedalaman benam alat, kelajuan perjalanan alat dan sudut kecondongan alat. Gabungan dinilai berdasarkan pencirian mikrostruktur mereka seperti zon kimpalan, ketebalan lapisan IMC, saiz butiran di zon bingkah dan sifat seperti kekerasan dan kekuatan tegangan. Kecacatan yang terbentuk pada sendi seperti kilat bahan yang berlebihan, ketidakcukupan pengikatan, kecacatan terowong dan kecacatan akar diteliti. Ketebalan lapisan IMC di bahagian atas dan tengah sendi diukur untuk semua sendi. Kedalaman benam alat ini dilihat sangat mempengaruhi penjanaan haba dan tekanan ke bawah, dibuktikan dengan penampilan kecacatan terowong pada 0.1 mm dan lapisan IMC tebal pada kedalaman benam 0.3 mm dan alat 0.5 mm alat. Pada kelajuan perjalanan alat (30 mm / min) yang sangat rendah (110 mm / min), kecacatan terowong telah terbentuk. Pada sudut kecondongan alat rendah iaitu  $1^\circ$ , kimpalan telah berjaya dilaksanakan. Lapisan IMC yang terbentuk dalam sendi adalah lebih nipis daripada yang di dalam sendi yang dihasilkan pada sudut kecondongan alat  $3^\circ$ , namun ia lebih tebal di bahagian paling atas sendi itu. Kecacatan akar diperhatikan dalam semua sendi yang dikimpal. Dengan membuang kecacatan akar dari spesimen tegangan beberapa sendi dengan pemesanan, kekuatan didapati sangat meningkat kerana retakan tidak lagi bermula pada kecacatan akar. Walau bagaimanapun, beberapa sendi tanpa kecacatan akar masih retak di antara muka, yang disebabkan oleh lapisan IMC yang tebal di puncak. FSW dwibelah (DS-FSW) disiasat sebagai kaedah yang mungkin dapat menghapuskan kecacatan akar tanpa penyingkiran bahan dengan pemesanan. Didapati bahawa dengan menggunakan DS-FSW yang memiliki panjang pin alat 4.5 mm dan 4.0 mm telah berjaya mengeluarkan kecacatan akar, namun sendi masih patah di antara muka. Didapati bahawa lapisan IMC tebal telah terbentuk di puncak sebelah pertama sendi. Sebaliknya, dengan melakukan DS-FSW menggunakan pin alat yang lebih pendek iaitu 3.5 mm dan 3.0 mm, kecacatan akar telah berjaya dikeluarkan dan retak sendi dari antara muka, menandakan sendi yang

memuaskan. Ketebalan lapisan IMC di sepanjang kedalaman sendi diukur untuk menyiasat kesan DS-FSW. Telah diperhatikan bahawa pin alat yang lebih panjang menghasilkan lapisan IMC yang lebih tebal dan sebaliknya.

@This item is protected by original copyright

## Parametric Investigation for Friction Stir Welding of Aluminum Alloy 6061-T6 and S275JR Mild Steel Butt Joint

### ABSTRACT

Friction stir welding (FSW) is a solid-state joining technique capable of joining aluminum and steel together, which is beneficial to multiple industries such as the automotive, aerospace and chemical industry is attributed by the combined high strength and toughness of steel as well as the corrosion resistance and low density of aluminum alloys. However, joining these two materials together has proven to be a difficult undertaking due to a strong tendency to form large amounts of brittle and hard intermetallic compounds (IMC) at the interface as a result of mutual diffusion during welding. While the growth of IMC layer is minimized in FSW due to the low process temperature, investigation on the influence of welding parameters on IMC layer formation as well as other joint properties such as tensile strength and hardness is required. The appearance of FSW-related joint defects such as tunnel defects, insufficient welding and root defects are also of interest due to its negative effect on joint strength. The influence of double sided FSW (DS-FSW) on joint properties of aluminum-to-steel joints as well as its ability to fix root defects also require evaluation. Several welding parameters were studied and their effects on joint properties investigated: tool offset, tool rotation direction, tool plunge depth, tool travel speed and tool tilt angle. Joints were evaluated based on their microstructural characterizations such as weld zones, IMC layer thickness, grain size in the stir zone and properties such as hardness and tensile strength. Defects formed on the joint such as excessive material flash, insufficient bonding, tunnel defect and root defect were scrutinized. The thickness of IMC layer at the top and middle region of the joint were measured for all joints. Tool plunge depth was seen to substantially influence heat generation and downwards pressure, evidenced by the appearance of tunnel defects at 0.1 mm and thick IMC layers at 0.3 mm and 0.5 mm tool plunge depth. At very low (30 mm/min) and very high (110 mm/min) tool travel speed, tunnel defects were formed. At 1° low tool tilt angle, welding was successfully performed. IMC layer formed in the joint was thinner than ones in a joint produced at 3° tool tilt angle, however at the topmost region of the joint it was thicker. Root defect was observed in all the welded joints. Removing the root defect from tensile specimens of several joints by machining was found to substantially increase the joint strength as fractures no longer initiate at the root defect. However, several joints without root defect still fractured at the interface, which was determined to be caused by thick IMC layer at the crown. Double sided FSW (DS-FSW) was investigated as a possible method to eliminate root defects without material removal by machining. It was found that using DS-FSW with a 4.5 mm and 4.0 mm tool pin length was successful in removing the root defect, however joints still fractured at the interface. It was found that thick IMC layers were formed at the 1<sup>st</sup> side crown of the joint. By performing DS-FSW using shorter tool pins of 3.5 mm and 3.0 mm, root defects were successfully removed and the joint fractured away from the interface, signifying satisfactory bonding. The IMC layer thickness along the depth of joints were measured to investigate DS-FSW's effects. It was observed that longer tool pins resulted in thicker IMC layer and vice versa.

## CHAPTER 1 : INTRODUCTION

### 1.1 Research Background

There is developing interest in dissimilar joining of two fundamental materials, iron and aluminum alloys. The various aluminum alloys offer excellent strength to weight ratio, high thermal conductivity, good corrosion resistance and acceptable formability. Steel on the other hand offers excellent strength, good corrosion resistance and toughness. The combination of steel's excellent strength and toughness with aluminum alloy's formability and lightness while at the same time maintaining proficient strength has the potential to satisfy the requirements for various industrial fronts. The combination improves the strength-to-weight ratio, which is attractive for the aerospace and automotive industry where there are ongoing demands to reduce vehicle weight, improve fuel efficiency and reduce fuel emission for pollution control (Dilthey & Stein, 2006; Sakiyama et al., 2013). In 2012, the Japanese automobile manufacturer, Honda utilized aluminum-to-steel joints in the front sub-frame of their flagship car "Accord 2013", which was inspired by the desire to reduce car weight, thus improving fuel efficiency (Kusuda, 2013). Steel and aluminum alloy joints are also gaining attention in shipbuilding and offshore construction for the purpose of reducing the weight of high speed vessels as well as achieving good marine corrosion, fire resistance and sound damping (Corigliano, Crupi, Guglielmino, & Mariano Sili, 2018). A dissimilar joint between aluminum alloys and steel also prove advantageous for several other industries; it has shown to provide high temperature corrosion protection for the chemical industry as well as to improve cooling efficiency in the cryogenic field (Fukumoto et al., 1997; Springer, Kostka, dos Santos, & Raabe, 2011; W. Xu, Liu, Luan, & Dong, 2009).

However, joining these two materials together has proven to be a difficult undertaking. This is mainly due to the highly different thermo-mechanical properties of the two materials, such as melting point, coefficient of thermal expansion, thermal conductivity and limited solid solubility. These incompatibilities make successfully manufacturing a sound joint between the aluminum alloy and steel a tough task. There is also a strong tendency to form large amounts of brittle and hard intermetallic compounds (IMC) at the interface as a result of mutual diffusion during welding (Ryabov, 1985). These brittle IMC will deleteriously impact the joint as it causes sudden failure during applied stress (Das, Basak, Das, & Pal, 2013; Movahedi, Kokabi, Reihani, Cheng, & Wang, 2013; Ogura et al., 2012). Several attempts to fabricate dissimilar joints between aluminum alloy and steel have been made to investigate the performance of various welding techniques such as explosion welding, ultrasonic welding and diffusion welding, however these techniques require high pressure, explosives or vacuum chamber, making it harder to be done inside assembly plants (Corigliano et al., 2018; Hussein, Tahir, & Hadzley, 2015; Kuroda, Saida, & Nishimoto, 1999; Lee, Yeon, Kim, & Jung, 2003; Tanaka T Morishige, 2009; Yamamoto, Takahashi, Ikeuchi, & Aritoshi, 2004).

Friction stir welding (FSW) was invented and patented by The Welding Institute (TWI) of Cambridge, UK in 1991 with its first works initially on aluminum alloys (Thomas, 1991). FSW is a solid-state joining technique that uses frictional heat generated between the tool shoulder and pin and the base metal, as well as adiabatic heat within the material. The processed materials will be plasticized at high temperatures without reaching the melting point. The weld is accomplished by plunging a rotating cylindrical tool along the weld joint. Friction stir welding is usually performed on a specialized FSW machine. A FSW machine is able to supply adequate torque and force, provide various controls on the rotating tool during the welding process such as rotational speed, traverse

speed, plunging rate and axial force measurement. Furthermore, FSW machines are also able to control the tool during the welding phase, such that it can be performed under several different modes such as displacement control and force control, as well as power control, torque control and temperature control on more advanced FSW machines. Even though FSW machines are excellent in terms of performance, its excessive cost means that its availability is restricted to advanced research and development institutes with sufficient funding. However, friction stir welding can still be performed on a milling machine with slight modifications to fit FSW purposes. By replacing the milling machine's cutting bit with a custom made tool bit, FSW can be performed.

FSW has garnered a lot of attention in several industries such as automotive, construction and aerospace for its many advantages (N. Kumar & Mishra, 2014). The process does not involve hazardous shielding gases and consumables, hence it is considered energy efficient and nature friendly (Carlone & Palazzo, 2015). Complications such as solidification cracking and porosity which are commonly encountered by conventional welding methods can also be avoided by FSW since it is a solid state welding technique. Most importantly, for the industries interested in joining aluminum alloy and steel, the lower process temperature associated with FSW can also reduce the formation of brittle IMCs which has been the main issue plaguing traditional fusion welding processes. Honda developed a robotized FSW technology to fabricate an aluminum-to-steel lap joint for its Accord 2013 sub-frame, hence becoming the first automotive industry to weld dissimilar materials for mass produced vehicles (Kusuda, 2013). The implementation of FSW in fabrication reduced weight, power consumption as well as improving rigidity. Due to the increased interest, over the years FSW has also expanded to several variations of the basic technology such as laser assisted FSW, gas tungsten arc welding (GTAW) assisted FSW, double sided FSW (DSFSW) and

underwater FSW (UFSW) (H. S. Bang, Bang, Song, & Joo, 2013; Fei, Jin, Ye, Xiu, & Yang, 2016; Rahimi, Wynne, & Baker, 2017; Wahid, Khan, & Siddiquee, 2018) . These variations were explored as means to overcome certain limitations of the basic FSW process (DS-FSW to weld thick steel plates) as well as improve joint properties (finer grains in UFSW joints as a result of lower process temperature).

Due to these advantages, there has been a lot of studies on FSW for dissimilar material joining. Barbini et al. investigated the FSW butt joint between two dissimilar aluminum alloys commonly used for aerospace manufacturing, AA2024-T4 and AA7050-T7651 using an variation of the FSW technology which utilizes a stationary shoulder (SSFSW) and discovered the reduced welding area by using SSFSW resulted in improved heat distribution, thus raising tensile strength (Barbini, Carstensen, & dos Santos, 2018). Zheng et al. investigated the FSW lap joint between two dissimilar materials, 2A70 aluminum alloy and Inconel 600 nickel alloy and produced successful joints, as well as discovered a thin  $Al_3Ni$  interlayer formed at the interface of the joints (Zheng, Feng, Shen, Huang, & Zhao, 2017).

The application of FSW to join aluminum alloy and steel has also been studied by several researchers. Chen and Kovacevic first explored the possibility of joining AA6061 and AISI 1018 steel in 2004 and discovered IMCs in the weld zone, as well as noting significant tool wear at higher tool offset towards steel, thus increasing tool interaction with steel side (C. M. Chen & Kovacevic, 2004). Since then, a number of investigations on joint properties were done by several researchers. One of the most cited papers in the field published by Dehghani et al. investigated the FSW joining between AA5186 and St 52 mild steel and discovered that IMC layer thickness, presence of joint defects and tensile strengths of joints depend on several welding parameter values and developed the

heat input factor (HIF) model to illustrate the relationship between tensile strength and various welding parameters (Dehghani, Amadeh, & Akbari Mousavi, 2013). One of the most recent papers in the field by Sheng Zhao et al. investigated the influence of tool size, tool offset and tool rotational speed on FSW joints between AA6061-T6511 and TRIP 780/800 steel and discovered that low heat generation from both low tool rotational speed and low tool interaction with steel side resulted in crack-like defects at the root of joints which deteriorated tensile strength of affected joints (S. Zhao et al., 2018). From these recent publications, it can be said that there is continuous interest in FSW in welding similar and dissimilar materials. In particular, the relationship between welding parameters such as tool rotational speed and tool travel speed with IMC layer thickness, joint defects and tensile strength are often studied.

In this thesis, FSW joints of two dissimilar materials AA6061-T6 and S275JR are investigated. AA6061-T6 was chosen for its excellent corrosion resistance and strength-to-weight ratio, while S275JR was selected for its good strength, toughness, formability and availability. Both materials are commonly available in Malaysia, therefore the joining of these two materials via FSW can be applied for the automotive and aircraft industry. The influence of several welding parameters on microstructural and mechanical properties as well as presence of joint defects are explored. In addition, this research aims to address the gap in knowledge regarding the influence of DS-FSW on aluminum alloy and steel joints. As DS-FSW has only been previously investigated on aluminum alloys, this research explores the feasibility of performing DS-FSW to join dissimilar materials (aluminum alloy and steel).

## 1.2 Problem Statement

It is feasible for FSW to be performed on a milling machine with slight modifications to fit FSW purposes. However, several functions available on the FSW machine are unavailable on the modified milling machine due to the difference in technology. Considering the much wider availability of milling machines in Malaysia, an evaluation of the FSW process using a conventional milling machine is desirable. Satisfactory FSW performance would mean that any workshop, industrial or academic, with a conventional belting milling machine will have the ability to weld aluminum alloy and steel.

From the dissimilar aluminum-to-steel FSW studies available in literature, it is apparent that different set of optimal parameters were obtained for different setups. For example, Ramachandran et al. found that the best tensile strength was obtained by the joint welded with tool rotational speed of 450 rpm, with tensile strength decreasing at higher tool rotational speeds (Ramachandran, Murugan, & Shashi Kumar, 2016). On the other hand, Xun Liu et al. was able to produce joints with satisfactory tensile strength even at tool rotational speeds up to 1800 rpm (X. Liu, Lan, & Ni, 2014). Dehghani et al. saw decreasing tensile strength when increasing the tool travel speed from 56 mm/min to 80 mm/min due to the appearance of tunnel defects, however Yazdipour et al. produced a satisfactory joint at 160 mm/min tool travel speed (Dehghani, Amadeh, et al., 2013; Yazdipour & Heidarzadeh, 2016). Similarly, Derazkola et al. discovered surface voids when increasing tool tilt angle from 2° to 3°, while Dehghani et al. only encountered issues when tool tilt angle was increased from 3° to 5° (Dehghani, Amadeh, et al., 2013; Derazkola, Aval, & Elyasi, 2015). Based on these examples and other researches in literature it can be seen that parameters behave differently for different setups which

might be caused by variations in material alloys and grades, tool design, tool material, material thickness as well as machine specifications. Therefore, there is a need to establish a set of parameters for a particular FSW setup that can produce satisfactory joints. It is also noted that while investigations have been performed on FSW joints of various aluminum alloy to steel grade combinations, a detailed investigation on AA6061-T6 and S275JR FSW joint is lacking. AA6061-T6 is sought after due to its excellent strength-to-weight ratio as well as its non-corrosive properties, while S275JR is a commonly used mild steel grade for its strength and shock resistance (Polmear, 1995). As both materials are commonly used in various industries, the FSW joint properties of these materials are of interest, particularly for the aircraft and automotive industries where vehicle weight and strength are important.

While aluminum alloys and steel joints are highly sought after by automotive, aerospace and chemical industries due to the improved strength-to-weight ratio and corrosion protection, joining these two materials together has proven to be difficult as thick and brittle IMC layers tend to form which severely weakened the resultant joint. Fabricating the joint with FSW was shown to reduce the IMC layer thickness due to lower process temperature, however it still remains a concern due to its brittle nature which could cause fast rupture under loading. Therefore, it is of paramount importance to investigate the IMC layer thickness for all joints, establish its relationship with the welding parameters and analyze its effects on joint strength. Additionally, the influence of welding parameters on the grain size in the stir zone as well as hardness of the joints are also of interest.

While IMC layer formation is the main issue with welding aluminum alloy and steel, the occurrence of joint defects native to the FSW process such as tunnel defect,

excessive flash, kissing bond and surface groove is also of interest due to its detrimental effect to a FSW joint (Khan et al., 2017; Podrzaj, Jerman, & Klobcar, 2015). Of these defects, tunnel defects and root defects (kissing bond, joint line remnant etc.) are difficult to detect with nondestructive methods, therefore these defects are of particular concern (Besel, Besel, Mercado, Kakiuchi, & Uematsu, 2016; Kadlec, Růžek, & Nováková, 2015; Khan et al., 2017). Khan et al. investigated tunneling and kissing bond defects in FSW between AA5083-H116 and AA6063-T6 and found that tunnel defects occurred when tool was offset towards stronger material, with its size depending on the offset value (Zaman, Noor, Khan, & Shihab, 2015). Kissing bonds were only successfully prevented at tool offset of 0.5 mm towards the weaker material and at high plunge depth. Kadlec et al. examined the kissing bond in FSW joints of similar AA7475 plates and found that kissing bonds with depths above 0.3 mm are harmful to the joint fatigue life (Kadlec et al., 2015). Zhou et al. investigated the effect of kissing bond on FSW of AA5083-H112 joints (Zhou et al., 2018). The authors found that increasing the heat input managed to reduce the length of kissing bond. Fracture along the kissing bond was found to be related to poor tensile and fatigue strength. A similar defect at the root was also observed in several studies of FSW between aluminum alloy and steel, which were referred to as “unwelded region” and “unstirred zone” (Dehghani, Amadeh, et al., 2013; Dehghani, Mousavi, & Amadeh, 2013; Uzun, Dalle Donne, Argagnotto, Ghidini, & Gambaro, 2005). However, it was noted that the respective researchers elected to machine away the defects as it was not within the scope of their investigation. The removing of material at root, while successful at removing root defects, might not be desirable in certain situations where wasting material and spending extra time and energy to remove material are not ideal. Thus, it is important to investigate the presence of these defects in joints and study

their relationship with the welding parameters, as well as analyze their impact on joint strength.

As root defects are difficult to detect, there is a need for a technique that is capable of solving this defect with machining it away as it costs time, wastes material and potentially introduces other defects during material removal. Double sided FSW (DS-FSW) is an innovation of the FSW technique that involves welding both sides of the joint, instead of only one side in the conventional FSW. As such, DS-FSW should be able to solve the root defect problem which is caused by a lack of bonding between the two plates at the root. There are several studies of DS-FSW on aluminum alloys available in literature, however there is a lack of existing dissimilar material DS-FSW studies, particularly in aluminum-to-steel joining. This might be due to the concern of 2<sup>nd</sup> side welding negatively affecting the IMC layer of the joint due to the additional heat exposure from 2 weld cycles. Therefore, it is desirable to investigate the feasibility of DS-FSW to fabricate an aluminum-to-steel joint using the DS-FSW method as well as to solve root defects. Furthermore, the influence of different tool pin lengths in DS-FSW on microstructure and mechanical properties of joints is also of paramount interest.

### **1.3 Objective**

The aim of this research work encapsulates the following objectives.

1. To evaluate the capability of performing FSW to join AA6061-T6 and S275JR in a butt joint on a conventional milling machine.
2. To investigate the influence of FSW welding parameters on microstructural properties such as IMC layer thickness, grain size and weld zones as well as mechanical properties such as hardness and tensile strength of an AA6061-T6 and S275JR FSW joint.

3. To identify the joint defects that occur at different sets of welding parameter values as well as analyze the relationship between welding parameters and joint defects such as excessive material flash, tunnel defect, insufficient bonding and root defects.

4. To investigate the feasibility of performing DS-FSW on an AA6061-T6 and S275JR FSW joint as a solution for root defect as well as to examine the influence of tool pin length on microstructural properties such as IMC layer thickness, grain size and weld zones as well as mechanical properties such as hardness and tensile strength.

#### **1.4 Scope of Work**

In this research, FSW was the technique used to produce butt joints between AA6061-T6 and S275JR plates of 5 mm thickness. A conventional milling machine equipped with a custom FSW tool made from H13 tool steel with 20 mm shoulder diameter and an unthreaded cylindrical pin of 5 mm diameter was used to produce joints.

The influence of welding parameters such as tool offset, tool rotation, tool plunge depth, tool travel speed and tool tilt angle on microstructural and mechanical properties were investigated, which include IMC layer, grain size, weld zones as well as hardness and tensile strength. Joint defects were also evaluated to investigate their correlation with welding parameters. Tensile strength of joints were evaluated, and its relationship with previous findings on microstructure and defects were studied.

DS-FSW was also performed to produce butt joints of AA6061-T6 and S275JR plates of 5 mm thickness using the same setup. In this study, the influence of different tool pin length on IMC layer, grain size, weld zones, hardness and tensile strength of joints were evaluated. Three hardness profiles were taken at different joint depths, while multiple regions of IMC layer on the interface of joints were analyzed to determine the

variation of said properties caused by DS-FSW. DS-FSW's effectiveness in solving root defect is determined by observing fracture of tensile specimen during tensile testing.

## **1.5 Organization of the Dissertation**

The first chapter gives a general overview of dissimilar material welding, their advantages and applications as well as issues pertaining to joining aluminum alloys and steel. The chapter also provides a brief introduction to FSW and its advantages in solving the problems related to joining dissimilar aluminum alloys and steel. This chapter also discusses the problem statements related to issues of aluminum-to-steel FSW, research objectives and scope of work.

The second chapter reviews previous works relevant to the FSW work in this study. Firstly, the basic principles and terminologies of FSW is introduced. Next, dissimilar aluminum-to-steel FSW works are reviewed. Recent advances in aluminum-to-steel FSW are presented as well as the findings of most relevant papers in the field. After that, defects and issues commonly seen in FSW joints are highlighted. The influence of FSW on microstructure of joints such as welding zones and grains as well as IMC layer for dissimilar aluminum-to-steel FSW are also reviewed. Finally, the advances of a subsection of FSW called double sided FSW is presented, highlighting its effects on various mechanical and microstructural properties.

The third chapter explains the materials used for the FSW as well experimental procedures and analysis techniques. The flow chart of research methodology is also presented here.

The first section in the fourth chapter presents the results of parametric study of AA6061-T6 and S275JR FSW butt joint. The influence of tool offset, tool rotation, tool

plunge depth, tool travel speed and tool tilt angle on microstructural properties, joint defects and microhardness are presented. The relationship between welding parameters and both defects and microstructure are also discussed and summarized. Next, the influence of defects and microstructure on tensile strength is presented. The second section in the fourth chapter discusses the influence of double sided FSW on AA6061-T6 and S275JR butt joints. Microstructural properties, joint defects, microhardness and tensile strength of DS-FSW joints welded with different tool pin lengths are investigated.

Finally, the fifth chapter focuses on the conclusions obtained from the results as well as the objectives met in this research. This chapter also provides suggestions for future researches in this area.

## CHAPTER 2 : LITERATURE REVIEW

This chapter provides a basic introduction to the FSW process as well as the commonly used terminologies pertaining to the field. It also reviews the literature available on the studies of FSW between aluminum alloys and steels. The review highlights the advantages of the application of FSW in joining the two dissimilar materials as well as the current applications in the industry. Next, a review of the common welding parameters of interest in aluminum-to-steel FSW studies are highlighted. Besides that, the influence of said welding parameters onto factors such as heat generation, material flow and material consolidation are reviewed.

Next, common defects seen in similar aluminum alloys and dissimilar aluminum-to-steel FSW joints are presented. Microstructural changes in an FSW joint such as the formation of welding zones and grain size are also reviewed. As IMC layers are a major concern in aluminum-to-steel joining, a review of the formation theory as well as the common chemical compositions seen in joints are included. IMC layer thickness seen across the various aluminum-to-steel FSW studies are also review.

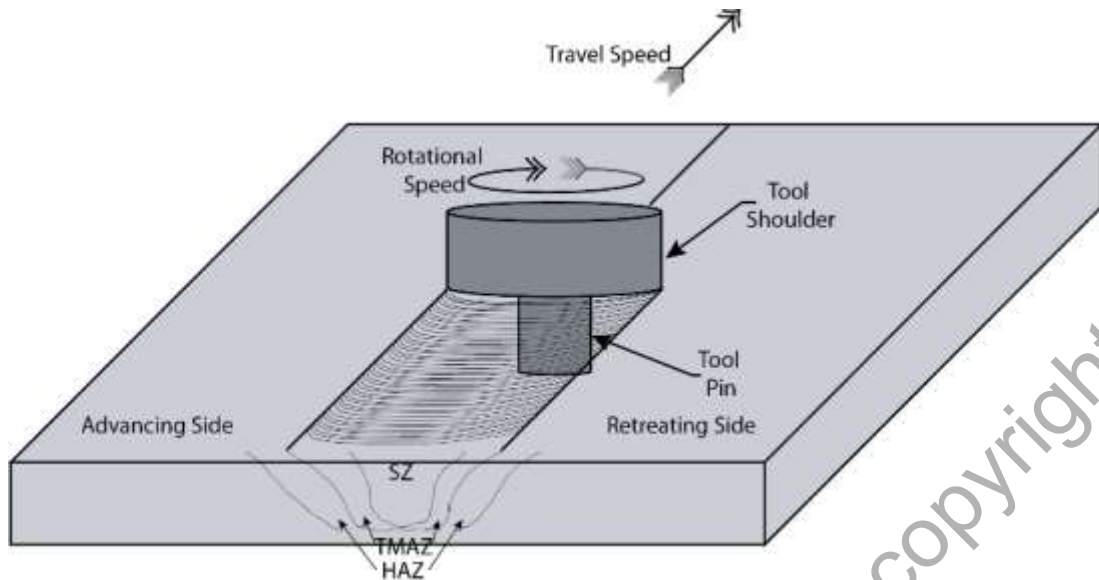
Finally, the current state of technology of DS-FSW is assessed in order to clarify current issues and focus in the field. The effect of DS-FSW on microstructural (welding zones, grain size) and mechanical properties (hardness, tensile) of joints is reviewed.

## 2.1 Friction Stir Welding

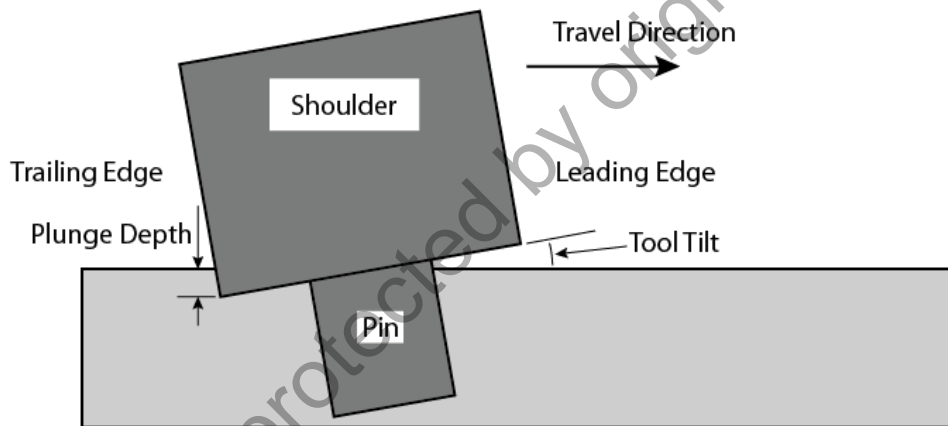
### 2.1.1 Introduction

Friction stir welding (FSW) was invented and patented by The Welding Institute of Cambridge, UK in 1991 with its first works initially on aluminum alloys (Thomas, 1991). FSW is a solid-state joining technique that uses frictional heat generated between the tool shoulder and pin and the base metal, as well as adiabatic heat within the material. The processed materials will be plasticized at high temperatures without reaching the melting point, i.e. “solid state”.

The weld is accomplished by plunging a rotating non-consumable cylindrical tool with special shoulder and pin of various designs. The tool is inserted in between the interface of two separate plates to be joined and afterwards is allowed to travel along the joint according to the weld configuration. The tool is responsible for providing the primary heat source for the welding process, facilitating the flow of plasticized material around the pin, and consolidating the plasticized material downwards beneath the tool shoulder (N. Kumar & Mishra, 2014; Y S Sato, Fujimoto, Abe, & Kokawa, 2008). Heat is created via friction between the rotating tool surface (shoulder and pin) and the weld pieces, as well as severe plastic deformation within the material (Colegrove, 2001; N. Kumar & Mishra, 2014). The frictional heat by the pin softens the material adjacent to it to a plasticized state. The plasticized material then experiences movement from front to back of the tool pin due to the rotation and travel displacement of the tool and eventually settles into the void left by the pin as it gets pushed down by the shoulder (N. Kumar & Mishra, 2014).



(a)



(b)

Figure 2.1 (a) Schematic diagram of friction stir welding. (b) Side view of schematic diagram

The schematic diagram in Figure 2.1 depicts a FSW tool traveling and rotating in the directions specified. The advancing side (AS) is defined as the material side placed where the travel velocity points in the same direction as the tangent of rotational velocity, whereas retreating side (RS) is the material placed where travel velocity is in the opposite direction of the tangent of rotational velocity (Thomas, 1991).

The tool seen here is a typical shoulder with an unthreaded cylindrical pin located at its bottom. Grooves can be added on the shoulder surface to enable better material flow inwards, therefore enhancing the tool's ability to retain plasticized material under the shoulder. Concave surface can also be added to the shoulder, also for the purpose of plasticized material containment. Convex surface is a bit rarer in use, but offers the versatility of welding pieces with different thickness. The tool pin is the first part of the tool to interact with the weld piece, thus is primarily responsible for initial heating of material to be plasticized as well as facilitating material flow both horizontally and vertically around the tool (Schmidt & Hattel, 2004). Several pin designs used include cylindrical, tapered, square, triangular and step spiral. Additions such as threads, flutes and flats can be done to further enhance material flow. It is very common for the tool to be tilted at certain angles. This is to improve material consolidation as well as downwards forging action by the shoulder (Dehghani, Amadeh, et al., 2013). The plunge depth is the distance from the weld piece surface to the bottom most surface of tool shoulder.

The leading and trailing edge are the front and back side of the tool respectively. At the leading edge, relatively colder material is moved towards the retreating side by the rotating tool shoulder. At the trailing edge, due to tool tilt and plunge depth, the majority of frictional heat between the tool shoulder and surface of weld pieces is generated (N. Kumar & Mishra, 2014). The trailing edge provides heat after initial pin interaction. Consolidation also occurs here as the shoulder pushes down plasticized material behind the pin.

For FSW in a butt and lap joint configuration, a typical welding run has four stages which are plunging, dwelling, welding (traveling) and retracting. During the plunging stage, the tool is gradually descended into the weld piece. Chipping usually occurs in the

beginning of this phase due to the cold state of both tool and weld piece. As the tool pin continues its descent deeper into the weld piece, temperature rises and more material adjacent to the pin gets softened and rises upwards. During the plunging stage, the axial force experienced by the tool is at the highest point due to the relatively low temperature of the weld piece compared to other stages, as can be seen in Figure 2.2 (X. Liu, Lan, & Ni, 2015). Careful consideration is taken during this stage to protect the tool pin from fracture, especially during welding very hard materials such as titanium and high strength low alloy (HSLA) steel. Eventually the plunging stage ends when the shoulder has achieved intimate contact with the weld piece surface. Dwelling stage begins here, where the tool is allowed to maintain the same position for a small period of time to allow the surrounding weld piece to achieve a suitable temperature for plastic flow. The welding stage begins after a while when sufficient temperature is achieved, where the tool travels along a direction to facilitate joining. The retracting stage is when the tool is lifted at the end of the weld, leaving a hole at the end.

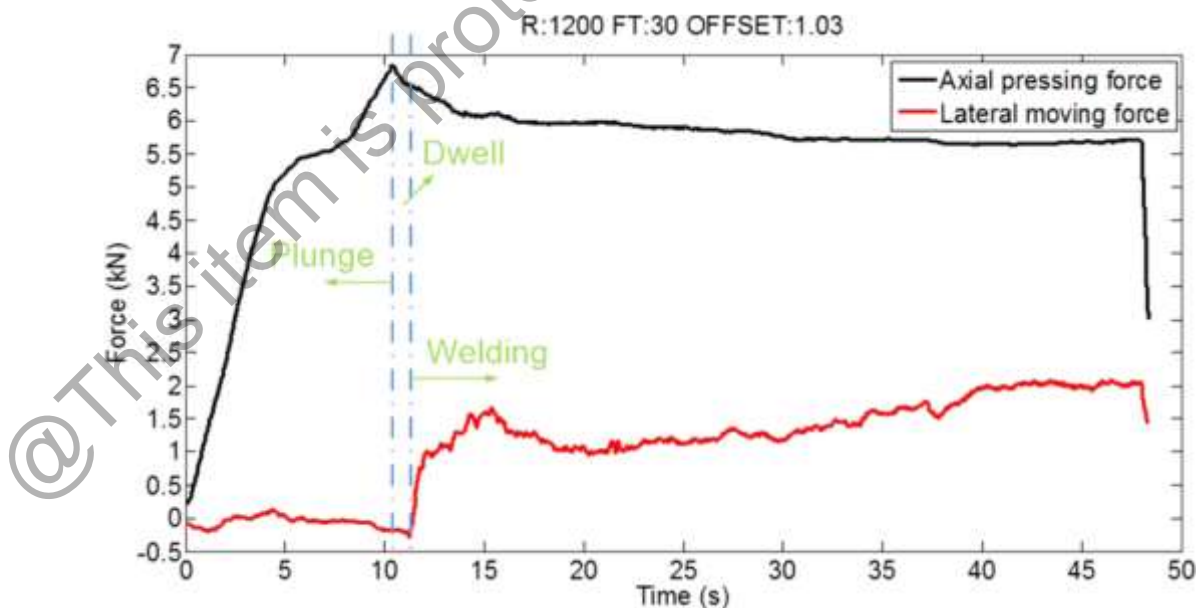


Figure 2.2 Axial pressing force and lateral moving force during plunging, dwelling and welding stages (X. Liu et al., 2015)

### 2.1.2 Zones

The FSW leaves distinct weld zones as a result of microstructural modifications, namely the stir zone (SZ), thermomechanically affected zone (TMAZ) and heat affected zone (HAZ) as shown in Figure 2.3. The SZ is usually seen with a size similar to the tool pin, and is characterized by the presence of very fine equiaxed grains produced through dynamic recrystallization as a result of severe plastic deformation and elevated temperature (Krasnowski, Hamilton, & Dymek, 2015). The SZ is usually shaped as basin-shaped or elliptical depending on tool design and welding parameters, and is sized similarly to the tool pin (Dehghani, Amadeh, et al., 2013; Mahoney, Rhodes, Flintoff, Bingel, & Spurling, 1998; Yutaka S Sato, Kokawa, Enomoto, & Jogan, 1999).

In the TMAZ, the weld pieces experiences plastic deformation and heat to a certain degree. However, no recrystallization occurred here due to insufficient deformation strain (Cabibbo, Forcellese, El Mehtedi, & Simoncini, 2014). Grains in this region are usually larger than in the SZ, owing to grain growth. In the HAZ, as suggested by its name, material here primarily experiences a thermal cycle from the tool shoulder. As this region is quite a distance away from the rotating pin, effects of plastic deformation are absent (Mishra & Ma, 2005). Grains are seen to be bigger than both SZ and TMAZ. Regions far away from the tool unaffected by deformation and significant heating have similar microstructural and mechanical properties to the base metal (BM).

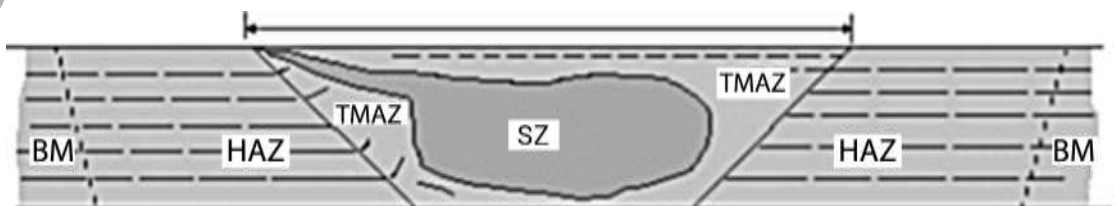


Figure 2.3 Cross sectional view of typical microstructure regions of a FSW joint (adapted from N. Kumar & Mishra, 2014)

### **2.1.3 Material flow at advancing side and retreating side**

In dissimilar FSW, the decision of placing materials at the advancing side or retreating side is significant as it affects material flow and mixing in addition to IMC formation (Izadi, Fallu, Abdel-Gwad, Liyanage, & Gerlich, 2013). At the leading edge, the rotation of tool shoulder produces a swiping mechanism to transfer materials from front to the back of the tool (Guerra, Schmidt, McClure, Murr, & Nunes, 2002). According to the Schneider-Nunes kinematic model, material at AS moves inwards towards tool pin, undergoes several cycles of material processing by the rotating pin then emerges at a height below its initial position, similar to a “whirlpool” pattern (Schneider & Nunes, 2004). On the contrary, material at RS experiences a “straight-through” current where it is simply deposited behind the tool without the downward movement for material at AS. It was shown by other researchers that performed simulations and experimental temperature measurements that in a similar FSW set up, temperature at AS tends to be higher than RS due to the difference in material flow (Cho, Boyce, & Dawson, 2007; Nandan, Debroy, & Bhadeshia, 2008; Nandan, Roy, Lienert, & Debroy, 2007)

### **2.1.4 Advantages of FSW**

FSW is a significant innovation in metal joining as it is considered a “green” technology, thanks to lower energy consumption, less dangerous emissions, no consumables involved, versatility and variability of fabricated joints. FSW made major advancements in joining aluminum alloys such as 2XXX and 7XXX series that were previously deemed impossible to joint using fusion welding techniques that existed prior to it. Additionally, FSW is also able to join dissimilar aluminum alloys and composites

(Y. Li, Murr, & McClure, 1999; Y. Li, Trillo, & Murr, 2000; Murr, Li, Flores, Trillo, & McClure, 1998).

Very fine equiaxed grains are obtained in the SZ of a FSW joint which leads to excellent mechanical properties. The solid state welding of FSW also means it avoids issues that commonly appear with conventional welding technique such as solidification cracking, porosity and slag inclusions. FSW also facilitates direct joining of materials without additional filler material. As such, it is also considered an economical process as the tool is non-consumable and no filler metal and shielding gas is required. The process is also relatively easy to perform compared to other conventional welding techniques which require a certain degree of skill in order to produce satisfactory joints. As FSW can be automated with the use of specialized FSW machines, the production time can be reduced.

Other than that, FSW is also considered a safe and environmentally friendly technology as no dangerous fumes are emitted during the process. The process temperature is also low, and there is no extreme brightness from the welding arc. The welder is also able to perform the welding in a more ergonomic way compared to other welding techniques. As FSW do not result in slag, the process eliminates grinding waste during slag removal.

#### **2.1.5 Current FSW innovations**

Over the past few years, several innovations of the FSW technology have appeared such as underwater FSW, ultrasound assisted FSW, friction stir dovetailing, stationary shoulder FSW, laser assisted FSW, multi-pass FSW and double sided FSW. In underwater FSW (UFSW), plates are submerged in water and the welding is facilitated

normally. Benefits of this method include lower peak temperature due to better heat absorption by water (Y. Zhao, Wang, Chen, & Yan, 2014). UFSW also resulted in better grain refinement in the SZ due to low maximum temperature and short period of exposure to high temperature (Sabari, Malarvizhi, & Balasubramanian, 2016; W F Xu, Liu, Chen, Luan, & Yao, 2012).

Stationary shoulder FSW is a combination of rotating pin and non-rotating shoulder that is allowed to slide over the weld piece surface during welding, which leads to minimal deformation and heat generation by the shoulder. It was shown to solve the temperature gradient issues that cause poor weldability in titanium alloy FSW (Ahmed, Wynne, Rainforth, & Threadgill, 2011). As the effect of shoulder on heat generation and plastic deformation is minimized, the width of SZ is reduced, the temperature distribution in the weld is improved which led to better hardness and microstructural homogeneity (Ji, Meng, Li, Ma, & Gao, 2016; D. Li, Yang, Cui, He, & Zhang, 2015). A variation to this method is the reverse dual rotation FSW (RDRFSW). The shoulder and pin are independent of each other, thus can rotate at different speed and direction. The tool shoulder and pin that rotate in opposite directions cancel each other out, reducing the net torque exerted onto both work piece and clamping jig (Shi, Wu, & Liu, 2015). Additionally, more homogeneous temperature distribution and microstructure across advancing side and retreating side was seen in RDRFSW joints, resulting in better weld integrity (Shi, Wu, & Liu, 2014).

There are also studies on hybrid techniques that incorporate FSW with other technologies. These are usually done to pre-heat the weld pieces prior to FSW. In dissimilar FSW between aluminum and steel, pre-heating is usually performed on the harder steel plate. GTAW-assisted FSW of AA6061-T6 and STS304 saw improved joint

efficiency, which was due to partial annealing and enhanced plastic flow of steel (H. Bang, Bang, Jeon, Oh, & Ro, 2012). Laser-assisted FSW of AA6016-T4 and DC04 steel allowed very high tool travel speed up to 2000 mm/min while maintaining good mechanical properties as well as high joint formability (Merklein & Giera, 2008). Furthermore, electrical current-assisted FSW of similar AA7075, AZ31B and high strength steel resulted in an increase of grain size in the AA7075 joint SZ, while grain refinement was improved for the AZ31B joint. Similar steel joint recorded high microhardness values at both sides of the joint (Luo, Chen, & Fu, 2014).

### **2.1.6 Tool design**

In terms of tool design, two of the most common material selections for tool fabrication are H13 tool steel and tungsten carbide (Hussein et al., 2015; Mishra & Ma, 2005). H13 tool steel is a very attractive choice due to its great fatigue strength and toughness as well as considerable strength at elevated temperatures at a good cost. Tools fabricated with tungsten carbide offer better fatigue strength at high temperatures, however it costs more to manufacture than the former (N. Kumar & Mishra, 2014).

In terms of tool geometry, based on literature review it was noted that tool pin length was usually 60% to 97% of the weld piece thickness (Coelho, Kostka, dos Santos, & Kaysser-Pyzalla, 2012; Ghosh, Gupta, & Husain, 2014; Kundu et al., 2013; X. Liu et al., 2014; Tanaka T Morishige, 2009). Pin length is kept less than the weld plate thickness to compensate for tool plunge depth as well as to keep the tool pin from coming in contact with the backing plate. Pin diameter was also found to be similar or larger than pin length, and no instance of pin diameter being smaller than pin length was observed (Kimapong & Watanabe, 2004; Tanaka T Morishige, 2009; Watanabe, Takayama, & Yanagisawa,

2006). Shoulder diameter was also commonly observed to be three to four times larger than the pin diameter (N. Kumar & Mishra, 2014).

## **2.2 FSW: Aluminum and Steel**

As a solid state process, FSW holds several advantages over conventional fusion welding techniques, such as the elimination of solidification cracking, slag inclusions and porosity (Sabari et al., 2016). For the industries interested in joining aluminum alloy and steel, lower process temperature associated with FSW can also reduce the formation of brittle IMCs which has been the main issue plaguing traditional fusion welding attempts (Ryabov, 1985; S. Zhao et al., 2018). Table 2.1 highlights the most commonly cited and relevant papers pertaining to friction stir welding of aluminum and steel in a butt joint configuration. Section 2.2.1 to Section 2.2.6 focuses on the influence of tool offset (TO), tool rotational speed ( $\omega$ ), tool travel speed (V), tool plunge depth (PD), tool tilt angle (TT) and tool rotation on joint properties.

Table 2.1 Most commonly cited aluminum-to-steel FSW papers

Year	Author	Materials Joined		At (mm)	St (mm)	Tool material	D <sub>S</sub> (mm)	D <sub>P</sub> (mm)	ω (rpm)	V (mm/min)	TO (mm)	PD (mm)	TT (°)	Findings
2004	Kovacevic	AA 6061	AISI 1018	6	6	Tool steel H13	25	5.5	914	140	-1.375	-	-	It is possible to FSW aluminum-to-steel. Tool broke at 100 mm into weld. Steel fragments in SZ.
2004	Kimapon	AA 5083	SS400	2	2	Tool steel SKH57	15	2	250	25	-0.2 to 0.2	-	-	Aluminum needs to be at AS. Steel fragments and interface serve as fracture paths. IMC mainly at upper part of interface.
2005	Uzun	AA 6013-T4	X5CrNi18-10 stainless steel	4	4		-	-	800	80	-	-	1	Root defect removed. Fatigue life 30% lower than Al BM.
2006	Watanabe	AA 5083	SS400	2	2	Tool steel	15	2	100 to 1250	25	-0.2 to 0.2	-	-	-0.2 mm best TO. Impossible to weld Aluminum at AS. Fracture follows steel fragments.